Chin. Ann. Math.
35B(3), 2014, 337–354
DOI: 10.1007/s11401-014-0837-9

Chinese Annals of Mathematics, Series B
© The Editorial Office of CAM and Springer-Verlag Berlin Heidelberg 2014

Adjoint Method for an Inverse Problem of CCPF Model*

Zhenhua CHEN[1] Kaiqi AN[1] Yuan LIU[1] Wenbin CHEN[2]

Abstract The problem for determining the exchange rate function of 2D CCPF model by measurements on the partial boundary is considered and solved as one PDE-constraint optimization problem. The optimal variant is the minimum of a cost functional that quantifies the difference between the measurements and the exact solutions. Gradient-based algorithm is used to solve this optimization problem. At each step, the derivative of the cost functional with respect to the exchange rate function is calculated and only one forward solution and one adjoint solution are needed. One method based on the adjoint equation is developed and implemented. Numerical examples show the efficiency of the adjoint method.

Keywords Adjoint method, Inverse problem, CCPF model, PDE-constraint optimization
2000 MR Subject Classification 35R30, 35K20

1 Introduction

Groundwater, being one of the most useful water sources in worldwide human society, meets one-third of the overall water needs in France and supplies up to 10%–15% of the water consumption in China. Among several different types of groundwater, karst aquifer should be mentioned here as one typical system. It mainly consists of the porous medium, referring to the matrix, which serves to hold the water. And in this system, some water conduits or pipes are embedded among the matrix which plays an important role in transporting the fluid flow and the contaminates.

For modeling the karst aquifers, the most used approach for geological studies is referred to as the coupled continuum pipe flow (CCPF, for short) model. The model is a coupled system consisting of a two-(2D, for short) or three-dimensional (3D, for short) continuum domain Ω_m, namely the matrix. The flow in matrix is governed by a Darcy-type system. Inside the matrix lies a one-dimensional (1D, for short) conduit Ω_c, which is governed by the pipe flow model. It was used in [2, 4, 15] to study the gensis of karst aquifers firstly. And the model, to some extent, reaches success. In the literature [14], a modified continuous CCPF model was proposed, which

Manuscript received October 25, 2013.
[1]School of Mathematical Sciences, Fudan University, Shanghai 200433, China.
E-mail: chenzhenhua@fudan.edu.cn akqballack@gmail.com 12110180072@fudan.edu.cn
[2]Corresponding author. School of Mathematical Sciences, Fudan University, Shanghai 200433, China.
E-mail: wbchen@fudan.edu.cn
*This work was supported by the Key Project National Science Foundation of China (No. 91130004), the Natural Science Foundation of China (Nos. 11171077, 11331004) and the National Talents Training Base for Basic Research and Teaching of Natural Science of China (No. J1103105).

was proved to be well-posed in the 2D case. Furthermore, Wang studied the well-posedness of the model in 3D case (see [19]).

In the CCPF model, the fluid exchange between the conduit and the matrix is calculated via an ad-hoc term $\alpha(h_m - h_c)$, where α is the exchange rate, and h_m and h_c are the hydraulic heads in the matrix and conduit, respectively. Chen et al pointed out that as long as the exchange rate was well selected, the relative error between the CCPF model and the Stokes-Darcy system could be less than 1% (see [9]), which implied the validity of the CCPF model in describing the fluid flows in karst aquifers as well as the significance of the exchange rate α. Since the discharge of the exchange flow varies in different locations, a precise description of the model entails α to be a function that depends on the horizontal variable x. For the forward problem, the well-posedness and regularity of the weak solution have been obtained in [8, 14, 17, 19]. And for the inverse problem, in [16], Lu et al firstly verified the uniqueness of the exchange rate and proposed an inverse problem of determining the exchange rate function α.

Usually, the inverse problem is often turned into one optimization problem and solved by the gradient-based method, which is generally considered to be accurate but inefficient (see [6, 18]). In this paper, we regard the inverse problem as a PDE-constraint optimization problem where the exchange rate function minimizes a functional that measures the error between the computed and measured data (see [13]). The solution of this constrained optimization problem is then accomplished by one gradient-based optimization algorithm that requires the computation of the derivative with satisfaction of the constraints. An auxiliary problem, called the adjoint problem, is solved in order to calculate the derivative efficiently. The so-called adjoint method has successfully applied in different fields (see [7, 11–12]). The forward and adjoint problems are solved by using efficient finite difference methods and iterative solvers. Similar technique has been used to reconstruct the interface of discontinuity in the conductivity (see [10]).

At each iteration of the optimization algorithm, the main computational cost of the derivative calculation is independent of the number of parameters used to represent the α since only the solutions of a forward problem and an adjoint problem are needed, a new search direction is calculated by the steepest descent update, and the exchange rate function is updated at each iteration by new search direction.

The rest of this paper is organized as follows. In Section 2, the framework of adjoint method for PDE-constraint optimization problem is presented. In Section 3, the froward problem and inverse problem of the CCPF model are introduced, and the adjoint gradient representation calculation and algorithm for the inverse problem are given in Section 4. Finally, numerical results verify the algorithm in Section 5.

2 Framework of Adjoint Method for PDE-Constraint Optimization Problem

In this section, the framework that will be used for reduced derivative computation is presented in a functional analytical setting (see [13]). We first transform the general optimization problem into a reduced optimization problem, then the optimality conditions and an adjoint based representation for the reduced gradient of the objective function are stated.

2.1 Optimization problem

Formally, we will consider one problem having the following form:

$$\min_{w\in W} J(w) \quad \text{s.t.} \quad E(w)=0, \quad c(w)\in\mathcal{K},\ w\in\mathcal{C}, \tag{2.1}$$

where $J:W\to\mathbb{R}$ is the objective function, $E:W\to Z$ and $c:W\to R$ are operators, W,Z,R are real Banach spaces, $\mathcal{K}\subset R$ is a closed convex cone, $\mathcal{C}\subset W$ is a closed convex set.

In general, W,Z and R are generalized function spaces and the operator equation $E(w)=0$ stands for a PDE or a system of coupled PDEs, constraint $c(w)\in\mathcal{K}$ is regarded as an abstract inequality constraint. In some cases, it is convenient to write $c(w)\in\mathcal{K}$ as the form of $w\in\mathcal{C}$, where $\mathcal{C}\subset W$ is a closed convex set, as a result, the inequality constraint is dropped:

$$\min_{w\in W} J(w) \quad \text{s.t.} \quad E(w)=0, \quad w\in\mathcal{C}. \tag{2.2}$$

For PDE-constraint problem, we will have one additional structure: Optimization variable w could be divided into two parts, a state $y\in Y$ and a control (or design) $u\in U$, where Y and U are Banach spaces. Then $W=Y\times U$, $w=(y,u)$, and the problem becomes

$$\min_{\substack{y\in Y\\ u\in U}} J(y,u) \quad \text{s.t.} \quad E(y,u)=0, \quad c(y,u)\in\mathcal{K}. \tag{2.3}$$

Here $y\in Y$ is described by $E(y,u)=0$ (usually a PDE). The control (or design) $u\in U$ is a parameter that shall be adapted in an optimal way.

2.2 Reduced problem and adjoint method

We consider again the optimal control (or design) problem of the form

$$\min_{\substack{y\in Y\\ u\in U}} J(y,u) \quad \text{s.t.} \quad E(y,u)=0, \quad (y,u)\in W_{\text{ad}}, \tag{2.4}$$

where $J:Y\times U\to\mathbb{R}$ is the objective function, $E:Y\times U\to Z$ is an operator between Banach spaces, $W_{\text{ad}}\subset W:=Y\times U$ is a nonempty closed set. Assuming that J and E are continuously Fréchet-differentiable, and for any $u\in U$, the state equation $E(y,u)=0$ has unique solution $y(u)\in Y$. Thus, we have a solution operator $u\in U\mapsto y(u)\in Y$. Furthermore, we assume that $E_y(y(u),u)\in\mathcal{L}(Y,Z)$ is continuously invertible, then the implicit function theorem ensures that $y(u)$ is continuously differentiable. By differentiating $E(y(u),u)=0$ with respect to u, we obtain an equation for $y'(u)$:

$$E_y(y(u),u)y'(u)+E_u(y(u),u)=0. \tag{2.5}$$

After inserting $y(u)$ into (2.4), we get one reduced problem:

$$\min_{u\in U} \widehat{J}(u):=J(y(u),u) \quad \text{s.t.} \quad u\in U_{\text{ad}}:=\{u\in U:(y(u),u)\in W_{\text{ad}}\}. \tag{2.6}$$

For the optimal problem, the computation of the derivative of the reduced objective function $\widehat{J}$ is very important. There are two methods to do this: one is the sensitivity approach, the other is the adjoint approach. For the sensitivity approach, the computational cost grows linearly with the dimension of U (see [13]).

2.2.1 Adjoint approach

In fact, there is one efficient way to compute the derivative of $\widehat{J}$. From

$$\begin{aligned}\langle \widehat{J}'(u), s\rangle_{U^*,U} &= \langle J_y(y(u),u), y'(u)s\rangle_{Y^*,Y} + \langle J_u(y(u),u), s\rangle_{U^*,U} \\ &= \langle y'(u)^* J_y(y(u),u), s\rangle_{U^*,U} + \langle J_u(y(u),u), s\rangle_{U^*,U},\end{aligned}$$

we see that $\widehat{J}'(u) = y'(u)^* J_y(y(u),u) + J_u(y(u),u)$. Consequently, the requirement of the operator $y'(u) \in \mathcal{L}(U,Y)$ can be weakened, and only the vector $y'(u)^* J_y(y(u),u) \in U^*$ is really required. By (2.5), $y'(u)^* J_y(y(u),u) = -E_u(y(u),u)^* E_y(y(u),u)^{-*} J_y(y(u),u)$, and by introducing an adjoint state $\lambda = \lambda(u) \in Z^*$, where $\lambda(u)$ solves the adjoint equation

$$E_y(y(u),u)^* \lambda = -J_y(y(u),u), \tag{2.7}$$

then $y'(u)^* J_y(y(u),u) = E_u(y(u),u)^* \lambda(u)$. So we have $\widehat{J}'(u) = E_u(y(u),u)^* \lambda(u) + J_u(y(u),u)$. The derivative $\mathrm{d}\widehat{J}(u,s) = \langle \widehat{J}'(u), s\rangle_{U^*,U}$ could be computed by the adjoint approach as follows:

1. For given u, we solve the state equation $E(y(u),u) = 0$, then we get the state variable $y(u)$.
2. By solving the adjoint equation (2.7), we get the adjoint variable $\lambda(u)$.
3. Compute $\mathrm{d}\widehat{J}(u,s) = \langle \widehat{J}'(u), s\rangle_{U^*,U}$ by

$$\mathrm{d}\widehat{J}(u,s) = \langle E_u(y(u),u)^* \lambda(u), s\rangle_{U^*,U} + \langle J_u(y(u),u), s\rangle_{U^*,U},$$

which is the adjoint gradient representation.

2.2.2 A Lagrangian-based view of the adjoint approach

The adjoint gradient representation could be derived in a more general way. For optimization problem (2.4), let us define Lagrange function $L : Y \times U \times Z^* \to \mathbb{R}$,

$$L(y,u,\lambda) = J(y,u) + \langle \lambda, E(y,u)\rangle_{Z^*,Z}.$$

Substituting $y = y(u)$ gives, for arbitary $\lambda \in Z^*$,

$$\widehat{J}(u) = J(y(u),u) = J(y(u),u) + \langle \lambda, E(y(u),u)\rangle_{Z^*,Z} = L(y(u),u,\lambda).$$

And differentiating the above equation gives

$$\langle \widehat{J}'(u), s\rangle_{U^*,U} = \langle L_y(y(u),u,\lambda), y'(u)s\rangle_{Y^*,Y} + \langle L_u(y(u),u,\lambda), s\rangle_{U^*,U}. \tag{2.8}$$

One special $\lambda = \lambda(u)$ can be chosen such that

$$L_y(y(u),u,\lambda) = 0. \tag{2.9}$$

This is the adjoint equation, actually, for one variational direction $d \in Y$,

$$\langle L_y(y,u,\lambda), d\rangle = \langle J_y(y,u), d\rangle_{Y^*,Y} + \langle \lambda, E_y(y,u)d\rangle_{Z^*,Z} = \langle J_y(y,u) + E_y(y,u)^* \lambda, d\rangle,$$

then $L_y(y(u),u,\lambda)=J_y(y(u),u)+E_y(y(u),u)^*\lambda$. According to (2.9), we obtain that

$$E_y(y(u),u)^*\lambda=-J_y(y(u),u).$$

By solving $E(y,u)=0$, we get y. Furthermore by solving adjoint equation $E_y(y(u),u)^*\lambda=-J_y(y(u),u)$, we get λ. By (2.8), the adjoint gradient representation reads

$$\widehat{J}'(u)=L_u(y(u),u,\lambda(u))=J_u(y(u),u)+E_u(y(u),u)^*\lambda(u). \tag{2.10}$$

2.3 Optimality conditions

Let us consider the problem (2.4). By the definition of $U_{\rm ad}$ in (2.6), the optimization problem is equal to $\min\limits_{(y,u)\in Y\times U} J(y,u)$ s.t. $E(y,u)=0,\ u\in U_{\rm ad}$. We introduce the following assumption.

Assumption 2.1 Assume that

1. $U_{\rm ad}\subset U$ is nonempty, convex and closed.
2. $J:Y\times U\to\mathbb{R}$ and $E:Y\times U\to Z$ are continuously Fréchet-differentiable, and U,Y,Z are Banach spaces.
3. For all $u\in U'_{\rm ad}$, there exists a neighborhood $U'_{\rm ad}$ of $U_{\rm ad}$, and $E(y,u)=0$ has a unique solution $y=y(u)\in Y$.
4. For all $u\in U'_{\rm ad}$, derivative $E_y(y(u),u)\in\mathcal{L}(Y,Z)$ is continuously invertible.

For the reduced problem (2.6), we have the following general result (see [7, 13]).

Theorem 2.1 *Assume Assumption* 2.1 *holds. If* $\overline{u}$ *is a local solution of the reduced problem* (2.6)*, then* $\overline{u}$ *satisfies the variational inequality*

$$\overline{u}\in U_{\rm ad},\quad \langle\widehat{J}'(u),u-\overline{u}\rangle_{U*,U}\geq 0,\quad \forall u\in U_{\rm ad}. \tag{2.11}$$

Next, we use the adjoint representation of derivative (2.10)

$$\widehat{J}'(u)=L_u(y(u),u,\lambda(u))=J_u(y(u),u)+E_u(y(u),u)^*\lambda(u),$$

where $\lambda(u)\in Z^*$ is the solution of the adjoint equation $E_y(y(u),u)^*\lambda=-J_y(y(u),u)$. Recalling the Lagrange function associated with (2.6) $L:Y\times U\times Z^*\to\mathbb{R}$,

$$L(y,u,\lambda)=J(y,u)+\langle\lambda,E(y,u)\rangle_{Z^*,Z},$$

we get the corollary of Theorem 2.1.

Corollary 2.1 *Let* $(\overline{y},\overline{u})$ *be an optimal solution of* (2.6) *and assume Assumption* 2.1 *holds. Then there exists an adjoint state* (*or Lagrange multiplier*) $\overline{\lambda}\in Z^*$*, such that the following conditions hold:*

$$E(\overline{y},\overline{u})=0, \tag{2.12}$$

$$E_y(\overline{y},\overline{u})^*\overline{\lambda}=-J_y(\overline{y},\overline{u}), \tag{2.13}$$

$$\overline{u}\in U_{\rm ad},\quad \langle J_u(\overline{y},\overline{u})+E_u(\overline{y},\overline{u})^*\overline{\lambda},u-\overline{u}\rangle_{U^*,U}\geq 0,\quad \forall u\in U_{\rm ad}. \tag{2.14}$$

Using Lagrange function, the above equations could be written in the compact form:

$$L_\lambda(\overline{y}, \overline{u}, \overline{\lambda}) = E(\overline{y}, \overline{u}) = 0, \tag{2.15}$$

$$L_y(\overline{y}, \overline{u}, \overline{\lambda}) = 0, \tag{2.16}$$

$$\overline{u} \in U_{\text{ad}}, \quad \langle L_u(\overline{y}, \overline{u}, \overline{\lambda}), u - \overline{u} \rangle_{U^*,U} \geq 0, \quad \forall u \in U_{\text{ad}}. \tag{2.17}$$

In this paper, we are interested in the numerical efficiency of the adjoint approach to solve the inverse problem, and do not want to verify Assumption 2.1, which can be verified in [13].

3 Analysis on the Mathematical Model

3.1 CCPF model

CCPF model is a coupled system consisting of a 2D or 3D continuum domain Ω_m, which stands for the matrix. There exists a 1D conduit Ω_c in the matrix, and the situation in the conduit is governed by pipe flow model. In practice, the matrix is soil or rock aquifers, the fluid exchanges between the matrix and the conduit (see Figure 1). In this paper, we assume that the matrix domain is $\Omega_m := (0, L) \times (-M, M)$, Ω_c is the conduit domain, and ν denotes the tangential direction along the 1D pipe/channel conduit.

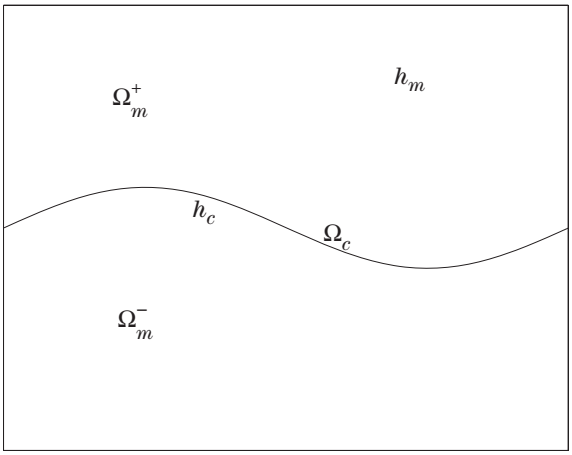

Figure 1 The geological description of the karst aquifers. h_m is the hydraulic head in the matrix, and h_c is the hydraulic head in the conduit $\Omega_m = \Omega_m^+ \cup \Omega_m^-$.

We first review the formulation of the coupled pipe flow/Darcy model. The flow in the porous matrix is modeled by Boussinesq equation (see [3]):

$$-\nabla \cdot (\mathbb{K} \nabla h_m) = S \frac{\partial h_m}{\partial t} - \gamma, \tag{3.1}$$

where h_m denotes the hydraulic head in the porous matrix, $\mathbb{K} \in \mathbb{R}^{2\times 2}$ is a hydraulic conductivity tensor. S is the storativity, and γ represents the volumetric rate of fluid transfering to the porous matrix from the conduit system per unit length.

For conduit flow, the discharge is related to the head difference in the tube by applying the Darcy-Weisbach equation (see [5])

$$Q = -D\frac{\partial h_c}{\partial \nu}, \tag{3.2}$$

where h_c is the hydraulic head in the conduit, Poisieulle constant $D = \frac{d^3 g}{12\rho}$, here d is the pipe diameter (channel width for 2D), Q is the total discharge in the pipe. Conversation of mass in the pipe implies $\frac{\partial Q}{\partial \nu} = -\gamma$, then we have $-\frac{\partial}{\partial \nu}\big(D\frac{\partial h_c}{\partial \nu}\big) = -\gamma$, The matrix and conduit flows are coupled at their intersection by the quasi-steady-state exchange term (see [8, 17, 19]),

$$\gamma = \alpha(h_c - h_m), \tag{3.3}$$

where $\alpha > 0$ is the exchange rate function, this means that the process in the conduit is enslaved by that in the porous matrix.

As a result, in the steady-state case, we have the system

$$\begin{cases} -\nabla\cdot(\mathbb{K}\nabla h_m) = -\alpha(h_m - h_c)\delta_{\Omega_c} + f_m & \text{in } \Omega_m, \\ -\dfrac{\partial}{\partial \nu}(D\dfrac{\partial h_c}{\partial \nu}) = \alpha(h_m|_{\Omega_c} - h_c) + f_c & \text{in } \Omega_c, \end{cases} \tag{3.4}$$

where h_m is the hydraulic head in matrix, h_c is the hydraulic head in conduit, δ_{Ω_c} is Dirac δ function concentrated on Ω_c, f_m and f_c represent the external source or sink. Laminar Poisieulle constant $D = \frac{d^3 g}{12\rho}$, where d is the diameter of the conduit, g is the earth's gravitational acceleration, and ρ is the kinematic viscosity of water, $\alpha(s) \in L^\infty_+(\Omega_c)$ is the exchange rate function where s denotes arc length variable.

3.2 Well-Posedness and regularity

Under the case of Dirichlet boundary condition, fixed hydraulic heads on the boundaries in both domains are introduced by

$$\begin{cases} h_m = g_m, & \partial\Omega_m, \\ h_c = g_c, & \partial\Omega_c, \end{cases} \tag{3.5}$$

where g_m and g_c are given a priori.

Define the space $\mathbf{H} := H^1_0(\Omega_m) \times H^1_0(\Omega_c)$(see [1]). We introduce a bilinear form as follows:

$$\begin{aligned} a(\mathbf{h},\mathbf{v}) : = &\int_{\Omega_m} \mathbb{K}\nabla h_m(x,y)\cdot\nabla v_m(x,y)\mathrm{d}x\mathrm{d}y + \int_{\Omega_c} D\frac{\partial h_c(s)}{\partial \nu}\frac{\partial v_c(s)}{\partial \nu}\mathrm{d}s \\ &+ \int_{\Omega_c} \alpha(s)(h_m|_{\Omega_c} - h_c(s))v_m(s)\mathrm{d}s - \int_{\Omega_c} \alpha(s)(h_m|_{\Omega_c} - h_c(s))v_c(s)\mathrm{d}s, \end{aligned} \tag{3.6}$$

where $\mathbf{h} = (h_m, h_c) \in \mathbf{H}$, and the test functions $\mathbf{v} = (h_m, h_c) \in \mathbf{H}$. Then for all $\mathbf{h} \in \mathbf{H}$, the weak solution of (3.4) $\mathbf{h}$ yields

$$a(\mathbf{h},\mathbf{v}) = \langle f_m, v_m\rangle_{L^2(\Omega_m)} + \langle f_c, v_c\rangle_{L^2(\Omega_c)}. \tag{3.7}$$

The following theorem shows that the weak solution uniquely exists under appropriate assumptions.

Theorem 3.1 *Assume that $f_m \in H^{-1}(\Omega_m)$, $f_c \in H^{-1}(\Omega_c)$ and $\alpha \in L^\infty_+(\Omega_c)$. Then the weak solution of* (3.4) $\mathbf{h}$ *uniquely exists, satisfying the following estimation:*

$$\|\mathbf{h}\|_{\mathbf{H}} \le C(\|f_m\|_{H^{-1}(\Omega_m)} + \|f_c\|_{H^{-1}(\Omega_c)}),$$

where C is a constant independent of f_m and f_c.

Higher regularity of the solution is possible, the proof of the theorem can be found in [8, 17, 19]. The well-posedness of the weak solution for Neumann boundary conditions is similarly compared with the Dirichlet boundary conditions.

3.3 Inverse problem of determining the exchange rate function α

In CCPF model, the fluid exchange rate between the matrix and the conduit is calculated by an ad-hoc term $\alpha(h_m|_{\Omega_c} - h_c)$, where $\alpha := \alpha(s)$ is the exchange function defined on the conduit domain Ω_c, and s stands for arc parameter. For anisotropic exchange rate function $\alpha(s) \in L^\infty_+$, Theorem 3.1 ensures the well-posedness of CCPF model. Now we discuss the uniqueness of the exchange rate by measuring the Cauchy data along one side of the boundary.

In the numerical realization, the geometry is described as following: The matrix Ω_m is a rectangle domain, $\Omega_m := (0, L)\times(-M, M)$, and the conduit Ω_c could be expressed by $y = \psi(x)$, where $\psi(x) \in C^2([0, L])$ and $\psi(0) = \psi(L) = 0$. Furthermore, we assume that the choice of $\psi(x)$ allows the well-posedness of the elliptic problem in a Lipschitz subdomain Ω'_m, where Ω'_m satisfies $\Omega'_m \subset \Omega_m$, $\partial\Omega'_m \cap \partial\Omega_m = \Gamma$, $\Omega_c \subset \Omega'_m$. Let $\Gamma := \{0\} \times (-M, M)$. The Cauchy data of partial boundaries of conduit domain Ω_c and matrix domian Ω_m are measured:

$$h_m(0, y)|_\Gamma = p(y)|_\Gamma, \tag{3.8}$$

$$\frac{\partial h_m(x, y)}{\partial x}\Big|_{x=0,\Gamma} = q(y)|_\Gamma, \tag{3.9}$$

$$h_c(0) = b, \tag{3.10}$$

$$\frac{\partial h_c(s)}{\partial \nu}\Big|_{s=0} = b_1. \tag{3.11}$$

Theorem 3.2 *Let us define $k(x) = \alpha(s(x))(h_m(x, \psi(x)) - h_c(s(x)))$. If there exist two functions $k_1(x)$ and $k_2(x)$ satisfying CCPF model*

$$\begin{cases} -\nabla\cdot(\mathbb{K}\nabla h_m) = -\alpha(h_m - h_c)\delta_{\Omega_c} + f_m & \text{in } \Omega_m, \\ -\dfrac{\partial}{\partial\nu}\Big(D\dfrac{\partial h_c}{\partial\nu}\Big) = \alpha(h_m|_{\Omega_c} - h_c) + f_c & \text{in } \Omega_c \end{cases}$$

with the same Cauchy data (3.8)–(3.11)*, there holds $k_1(x)$=$k_2(x)$ almost everywhere.*

The proof of the theorem can be found in [16]. In addition, if $k(x) = \alpha(s(x))(h_m(x, \psi(x)) - h_c(s(x)))$, let us define

$$\begin{cases} \alpha(s(x)) = \alpha_0, \quad \alpha_0 \text{ is a positive constant}, \quad \text{if } h_m(x, y)|_{\Omega_c} = h_c(s(x)), \\ \alpha(s(x)) = \dfrac{k(x)}{h_m(x, y)\delta_{\Omega_c} - h_c(s(x))}, \quad \text{else.} \end{cases}$$

Under some assumptions, if there exist two exchange rate functions $\alpha_1(s)$ and $\alpha_2(s)$ having the same Cauchy data (3.8)–(3.11), there holds $\alpha_1(s)$=$\alpha_2(s)$ almost everywhere (see [16]).

Then the inverse problem could be expressed as follows: if the Cauchy data are given on partial boundaries of matrix and conduit, we try to find an exchange rate function $\alpha(s)$ such that the associated weak solution $\mathbf{h}$ equals to the Cauchy data on the partial boundary.

4 Adjoint Method for Inverse Problem of CCPF Model

The inverse problem of CCPF model can be posed as optimization problem with the constraint given by a variational equation. The cost functional is the mismatch between the state obtained from a trial solution and the measured one:

$$J(\mathbf{h},\alpha)=\frac{1}{2}\|h_m-h_d^m\|^2_{L^2(\Omega_1)}+\frac{1}{2}\|h_c-h_d^c\|^2_{L^2(\Omega_2)}+\frac{\gamma^2}{2}\|\alpha\|^2_{\mathcal{H}(\Omega_c)},$$

where Ω_1 and Ω_2 are the parts of $\partial\Omega_m$ and $\partial\Omega_c$, respectively. Let $\mathbf{h}_d=(h_d^m,h_d^c)$ be the measured data and $\mathbf{h}=(h_m,h_c)$ the weak solution of (3.4). For instance, let us consider the Neumann boundary conditions:

$$(\mathbb{K}\nabla h_m)\cdot\boldsymbol{n}|_\Gamma=q(y)|_\Gamma, \tag{4.1}$$

$$(\mathbb{K}\nabla h_m)\cdot\boldsymbol{n}|_{\Gamma_1}=q_1(y)|_{\Gamma_1}, \tag{4.2}$$

$$D\frac{\partial h_c(s)}{\partial\nu}\Big|_{s=0}=b_1, \tag{4.3}$$

$$D\frac{\partial h_c(s)}{\partial\nu}\Big|_{s=S}=b_2, \tag{4.4}$$

where $\Gamma_1:=L\times(-M,M)$ is the right boundary of Ω_m, and S is the length of Ω_c (see Figure 2).

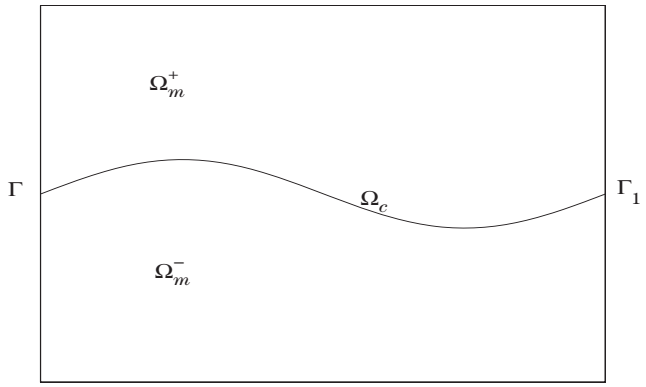

Figure 2 Domain and boundaries.

Usually, we consider the no flow boundary condition at $y=\pm M$,

$$(\mathbb{K}\nabla h_m)\cdot\boldsymbol{n}|_{y=M}=0,$$

$$(\mathbb{K}\nabla h_m)\cdot\boldsymbol{n}|_{y=-M}=0.$$

The physical background for this particular Neumann condition is that we assume there is no flows through the matrix on the upper and lower boundaries.

Define the space $\overline{\mathbf{H}}:=H^1(\Omega_m)\times H^1(\Omega_c)$. The weak formulation is now: finding $\mathbf{h}\in\overline{\mathbf{H}}$ such that

$$\begin{aligned}a(\mathbf{h},\mathbf{v})=&\langle f_m,v_m\rangle_{L^2(\Omega_m)}+\langle f_c,v_c\rangle_{L^2(\Omega_c)}+\langle q,v_c\rangle_{L^2(\Gamma)}+\langle q_1,v_c\rangle_{L^2(\Gamma_1)}\\&+(b_2h_c(S)-b_1h_c(0)),\quad\forall\mathbf{v}\in\overline{\mathbf{H}},\end{aligned}\tag{4.5}$$

which is one PDE-constraint. Consequently, solving the inverse problem equals to solving an optimization problem with the PDE-constraint,

$$\min_{\substack{\mathbf{h}\in\mathbf{H}\\ \alpha\in L^\infty_+(\Omega_c)}}\ J(\mathbf{h},\alpha)\quad\text{s.t.}\quad E(\mathbf{h},\alpha)=0,\quad(\mathbf{h},\alpha)\in W_{\rm ad}.\tag{4.6}$$

Define the spaces

$$\mathbf{Z}:=H^{-1}(\Omega_m)\times H^{-1}(\Omega_c),\quad\mathbf{Z}^*:=H^1(\Omega_m)\times H^1(\Omega_c).\tag{4.7}$$

Then the weak formulation (4.5) is equivalent to: finding $\mathbf{h}\in\overline{\mathbf{H}}$ such that

$$\begin{aligned}&\langle\mathbf{v},E(\mathbf{h},\alpha)\rangle_{\mathbf{Z}^*,\mathbf{Z}}\\&=\int_{\Omega_m}\mathbb{K}\nabla h_m(x,y)\cdot\nabla v_m(x,y)\mathrm{d}x\mathrm{d}y+\int_{\Omega_c}D\frac{\partial h_c(s)}{\partial\nu}\frac{\partial v_c(s)}{\partial\nu}\mathrm{d}s\\&\quad+\int_{\Omega_c}\alpha(s)(h_m|_{\Omega_c}-h_c(s))v_m(s)\mathrm{d}s\\&\quad-\int_{\Omega_c}\alpha(s)(h_m|_{\Omega_c}-h_c(s))v_c(s)\mathrm{d}s-\int_{\Omega_m}f_mv_m\mathrm{d}x\mathrm{d}y-\int_{\Omega_c}f_cv_c\mathrm{d}s\\&\quad-\int_{\Gamma}qv_m|_{x=0}\mathrm{d}x\mathrm{d}y-\int_{\Gamma_1}q_1v_m|_{x=L}\mathrm{d}s-(b_2h_c(S)-b_1h_c(0))=0,\quad\forall\mathbf{v}\in\mathbf{Z}^*.\end{aligned}\tag{4.8}$$

The formulation now defines the state equation operator

$$E:\{(\mathbf{h},\alpha):\mathbf{h}\in\overline{\mathbf{H}},\alpha\in W_{\rm ad}\}\to\{z:z\in\mathbf{Z},\alpha\in W_{\rm ad}\}.$$

Thus, we can define the reduced problem

$$\min_{\alpha\in\mathcal{A}_{\rm ad}}\widehat{J}(\alpha):=J(\mathbf{h}(\alpha),\alpha)\quad\text{s.t.}\quad\alpha\in\mathcal{A}_{\rm ad}:=\{\alpha\in\mathcal{A}:(\mathrm{h},\alpha)\in W_{\rm ad}\}.\tag{4.9}$$

4.1 Calculation of the gradient

From the adjoint gradient representation (2.10), we have to compute the Lagrange multiplier $\boldsymbol{\lambda}=(\lambda_m,\lambda_c)\in\mathbf{Z}^*$ by solving the adjoint system (2.7), which reads as

$$\langle\boldsymbol{\lambda},E_{\mathbf{h}}(\mathbf{h},\alpha)(\boldsymbol{\omega})\rangle_{\mathbf{Z}^*,\mathbf{Z}}=-\langle J_{\mathbf{h}}(\mathbf{h},\alpha),\boldsymbol{\omega}\rangle_{\overline{\mathbf{H}}^*,\overline{\mathbf{H}}},\quad\forall\omega\in\overline{\mathbf{H}}$$

with the given weak solution $\mathbf{h}$ of the state equation. The partial derivative $E_{\mathbf{h}}$ with respect to $\mathbf{h}$ is Fréchet derivative with the direction of $\boldsymbol{\omega} = (\omega_m, \omega_c)$. For the forward problem (4.8), the adjoint equation is: for all $\omega \in \overline{\mathbf{H}}$,

$$\int_{\Omega_m} \mathbb{K}\nabla\omega_m(x,y)\cdot\nabla\lambda_m(x,y)\mathrm{d}x\mathrm{d}y + \int_{\Omega_c} D\frac{\partial\omega_c(s)}{\partial\nu}\frac{\partial\lambda_c(s)}{\partial\nu}\mathrm{d}s + \int_{\Omega_c}\alpha(s)(\omega_m|_{\Omega_c} - \omega_c(s))\lambda_m(s)\mathrm{d}s - \int_{\Omega_c}\alpha(s)(\omega_m|_{\Omega_c} - \omega_c(s))\lambda_c(s)\mathrm{d}s = -\langle J_{\mathbf{h}}(\mathbf{h},\alpha),\omega\rangle_{\overline{\mathbf{H}}^*,\overline{\mathbf{H}}}, \tag{4.10}$$

where $\langle J_{\mathbf{h}}(\mathbf{h},\alpha),\omega\rangle_{\overline{\mathbf{H}}^*,\overline{\mathbf{H}}} = \int_{\Omega_m}(h_m - h_d^m)\delta_{\Omega_1}\omega_m\mathrm{d}x\mathrm{d}y + \int_{\Omega_c}(h_c - h_d^c)\delta_{\Omega_2}\omega_c\mathrm{d}x\mathrm{d}y$.

If $\Delta\alpha$ is the variational direction of the derivative, then

$$\langle \mathbf{v}, E_\alpha(\mathbf{h},\alpha)\Delta\alpha\rangle_{Z^*,Z} = \int_{\Omega_c}(h_m|_{\Omega_c} - h_c(s))v_m(s)\Delta\alpha\mathrm{d}s - \int_{\Omega_c}(h_m|_{\Omega_c} - h_c(s))v_c(s)\Delta\alpha\mathrm{d}s. \tag{4.11}$$

We consider an objective functional of the type

$$J(\mathbf{h},\alpha) = \frac{1}{2}\|h_m - h_d^m\|^2_{L^2(\Omega_1)} + \frac{1}{2}\|h_c - h_d^c\|^2_{L^2(\Omega_2)} + \frac{\gamma^2}{2}\|\alpha\|^2_{L^2(\Omega_c)}. \tag{4.12}$$

If $\Delta\alpha$ is the variaitonal direction of α, then

$$\langle J_\alpha(\mathbf{h},\alpha),\Delta\alpha\rangle_{\mathcal{A}^*,\mathcal{A}} = \int_{\Omega_c}\gamma\alpha\Delta\alpha\mathrm{d}s. \tag{4.13}$$

Finally, we get the adjoint gradient representation

$$\begin{aligned}\langle \widehat{J}'(\alpha),\Delta\alpha\rangle &= \langle J_\alpha(\mathbf{h},\alpha),\Delta\alpha\rangle_{\mathcal{A}^*,\mathcal{A}} + \langle\boldsymbol{\lambda}, E_\alpha(\mathbf{h},\alpha)\Delta\alpha\rangle_{Z^*,Z}\\ &= \int_{\Omega_c}(h_m|_{\Omega_c} - h_c(s))\lambda_m(s)\Delta\alpha\mathrm{d}s - \int_{\Omega_c}(h_m|_{\Omega_c} - h_c(s))\lambda_c(s)\Delta\alpha\mathrm{d}s\\ &\quad + \int_{\Omega_c}\gamma\alpha\Delta\alpha\mathrm{d}s.\end{aligned} \tag{4.14}$$

4.2 Optimization algorithm

Practically, the optimal variable $\alpha(s)$ is defined by the design parameter $u \in U$ with a finite or infinite dimensional design space U. Thus, we have a map $\alpha : u \to \alpha(u)$. Using the chain rule, derivatives of the objective function $\widehat{J}$ are obtained as

$$\left\langle \frac{\mathrm{d}}{\mathrm{d}u}\widehat{J}(\alpha),\cdot\right\rangle_{U^*,U} = \langle \widehat{J}'(\alpha),\alpha_u(u)\cdot\rangle_{U^*,U}. \tag{4.15}$$

If the design space of $\alpha(s)$ is finite dimensional, $\alpha(s) = \sum_{i=1}^{d}\phi_i(s)\alpha_i$, where $(\phi_1,\cdots,\phi_d)$ is a basis of design space U, and then $\widehat{J}'_u(\alpha(u))\cdot V = \sum_{i=1}^{d} G(\mathbf{h},\boldsymbol{\lambda},\phi_i)V_i$, with $G(\mathbf{h},\boldsymbol{\lambda},\phi_i) = \langle\widehat{J}'(\alpha),\phi_i\rangle$, where $\mathbf{h}$ and $\boldsymbol{\lambda}$ are solutions of the state equation and the adjoint equation, respectively, $G_i = G(\mathbf{h},\boldsymbol{\lambda},\phi_i)$ is the element of the gradient, and will be supplied to an optimization algorithm which is used in the solution of the inverse problem. For example, for the steepest decent method, we have the following algorithm.

Algorithm 4.1 (Steepest Decent Method) Choose an initial vector $u^0 = (\alpha_1^0, \cdots, \alpha_d^0)$ associated with the initial guess $\alpha^0(s)$.

For $k = 0, 1, 2, \cdots$,

1. If $\widehat{J}'(u^k) = 0$, STOP.
2. Choose a descent direction $d^k \in U$, such that $\langle \widehat{J}'_u(u^k), d^k \rangle_{U^*,U} < 0$: $d^k = -(G_1, \cdots, G_d)^{\mathrm{T}}$.
3. Choose a step size $\sigma_k > 0$ such that $\widehat{J}(u^k + \sigma_k d^k) < \widehat{J}(u^k)$.
4. Set $u^{k+1} := u^k + \sigma_k d^k$.

In our numerical experiments, the step size rule we used here is the Armijo rule.

Armijo Rule Given a descent direction $\Delta\alpha$ of $\widehat{J}$, choose the maximum $\zeta \in \{1, \frac{1}{2}, \frac{1}{4}, \cdots\}$ for which

$$\widehat{J}(\alpha + \zeta\Delta\alpha) - \widehat{J}(\alpha) \le \gamma\zeta\langle \widehat{J}'(\alpha), \Delta\alpha \rangle,$$

where $\gamma \in (0, 1)$ is a constant.

On the other hand, the descent direction $\Delta\alpha$ could be chosen by a special rule.

Lemma 4.1 *If $\mathcal{A}$ is a Hilbert space, $b(\cdot, \cdot)$ is a uniformly bounded and coercive bilinear form in $\mathcal{A}$ that satisfies*

$$b(\phi, \phi) \ge \alpha_0 \|\phi\|_{\mathcal{A}}^2, \quad \forall \phi \in \mathcal{A}, \tag{4.16}$$

$$b(\phi, \varphi) \le \beta_0 \|\phi\|_{\mathcal{A}} \|\varphi\|_{\mathcal{A}}, \quad \forall \phi, \varphi \in \mathcal{A}, \tag{4.17}$$

where $\alpha_0, \beta_0 > 0$, and $\Delta\alpha$ satisfies

$$b(\Delta\alpha, \phi) = -\langle \widehat{J}'(\alpha), \phi \rangle_{\mathcal{A}}, \quad \forall \phi \in \mathcal{A},$$

then it is guaranteed that $\zeta\Delta\alpha$ decreases the cost functional J, where ζ is a small enough positive number.

Proof From the definition, for any $\Delta\alpha \in \mathcal{A}$,

$$\langle \widehat{J}'(\alpha), \Delta\alpha \rangle = \lim_{\zeta \to 0} \frac{1}{\zeta} (\widehat{J}(\alpha + \zeta\Delta\alpha) - \widehat{J}(\alpha))$$

and

$$\begin{aligned} \widehat{J}(\alpha + \zeta\Delta\alpha) &= \widehat{J}(\alpha) + \langle \widehat{J}'(\alpha), \zeta\Delta\alpha \rangle + o(\zeta) \\ &= \widehat{J}(\alpha) - b(\Delta\alpha, \zeta\Delta\alpha) + o(\zeta) \\ &\le \widehat{J}(\alpha) - \alpha_0 \zeta \|\Delta\alpha\|^2 + o(\zeta). \end{aligned}$$

Indeed, the second term on the right side of inequality is strictly negative and the third term can be chosen such that $\lim\limits_{\zeta \to 0} \frac{1}{\zeta} o(\zeta) = 0$.

Theorem 4.1 (Choice of the Descent Direction) *If* $\mathbf{h} = (h_m, h_c)$ *is the weak solution of* (4.8), $\boldsymbol{\lambda} = (\lambda_m, \lambda_c)$ *is the weak solution of adjoint equation* (4.10), *then we can choose*

$$\Delta\alpha = -(h_m|_{\Omega_c-} - h_c)(\lambda_m|_{\Omega_c-} - \lambda_c) - \gamma\alpha$$

such that

$$\widehat{J}(\alpha + \zeta\Delta\alpha) < \widehat{J}(\alpha),$$

where ζ *is small enough. Choice of* ζ *could use the Armijo rule.*

Proof From Lemma 4.1, the bilinear form is $b(\Delta\alpha, \phi) = \langle\Delta\alpha, \phi\rangle$, and obviously it satisfies (4.16)–(4.17). The adjoint gradient representation gives

$$\begin{aligned}\langle\widehat{J}'(\alpha), \phi\rangle &= \langle J_\alpha(\mathbf{h}, \alpha), \phi\rangle_{\mathcal{A}^*,\mathcal{A}} + \langle\boldsymbol{\lambda}, E_\alpha(\mathbf{h}, \alpha)\phi\rangle_{Z^*,Z}\\ &= \int_{\Omega_c}((h_m|_{\Omega_c-} - h_c)(\lambda_m|_{\Omega_c-} - \lambda_c) + \gamma\alpha)\phi\mathrm{d}s.\end{aligned}$$

Because of the choice of the $\Delta\alpha$,

$$b(\Delta\alpha, \phi) = -\langle\widehat{J}'(\alpha), \phi\rangle_{\mathcal{A}}, \quad \forall\phi \in \mathcal{A},$$

we get

$$\Delta\alpha = -(h_m|_{\Omega_c-} - h_c)(\lambda_m|_{\Omega_c-} - \lambda_c) - \gamma\alpha.$$

5 Numerical Results

In this section, we demonstrate the adjoint derivative calculus on a numerical model problem. We choose the decent direction $\Delta\alpha(s)$ by Theorem 4.1. Numerical results show the efficiency.

5.1 Problem description

For convenience and simplicity, the computational domain in the model is the matrix domain $\Omega_m := [0, 1] \times [-1, 1]$ with the upper section $\Omega_m^+ = [0, 1] \times [0, 1]$ and the lower section $\Omega_m^- = [0, 1] \times [-1, 0]$, and the conduit domain is $\Omega_c = [0, 1] \times \{0\}$ (see Figure 3).

We begin to construct one exact solution of the model with a target exchange rate function, for convenience of numerical experiments, the hydraulic conductivity tensor $\mathbb{K}$ is set to be $\mathbb{I}$, and the Poisieulle constant D is set to be 1. Furthermore, considering the fact that the domain Ω_c is a straight line in the experiments, the CCPF model in this section is

$$\begin{cases}-\Delta h_m = -\alpha(h_m - h_c)\delta_{\Omega_c} + f_m & \text{in } \Omega_m,\\ -\dfrac{\mathrm{d}^2 h_c}{\mathrm{d}x^2} = \alpha(h_m|_{\Omega_c-} - h_c) + f_c, & \text{in } \Omega_c.\end{cases} \tag{5.1}$$

We adjust the forcing f_m and f_c in Ω_m and Ω_c, respectively, such that the exact solution is

$$\begin{cases}h_c = 2\sin(\pi x) & \text{in } \Omega_c,\\ h_m = \sin(\pi x) & \text{in } \Omega_m^-,\\ h_m = (-(2 + \sin(\pi x))y + 1)\sin(\pi x) & \text{in } \Omega_m^+.\end{cases}$$

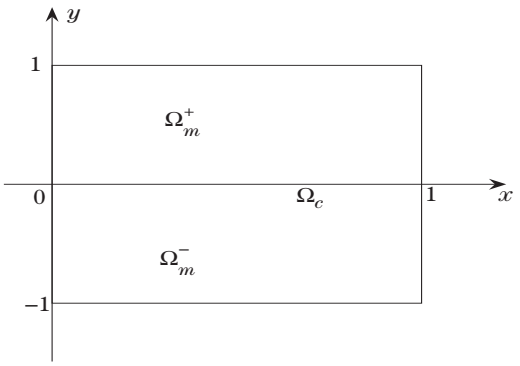

Figure 3 Computational domain in the numerical examples.

As a result, the target exchange rate function is $2+\sin(\pi x)$, f_m and f_c in (5.1) are

$$\begin{cases} f_c = 2\pi^2 \sin(\pi x) + (2+\sin(\pi x))\sin(\pi x) & \text{in } \Omega_c, \\ f_m = \pi^2 \sin(\pi x) & \text{in } \Omega_m^-, \\ f_m = y(-2\pi^2 \sin(\pi x) + 2\pi^2 \cos(2\pi x)) + \pi^2 \sin(\pi x) & \text{in } \Omega_m^+. \end{cases}$$

5.2 Convergence of the finite difference method

For the forward problem and the adjoint problem, we use finite difference method to solve them. Here we present the convergence of the finite difference method, i.e., we will prove that the numerical approach is accurate for solving the partial differential equation systems. We compute the finite difference approximation by using the sequence of grid sizes $h = 2^k, k = 1, \cdots, 6$. Errors are measured by the discrete l^2 norm.

Definition 5.1 *The convergence factor is given as convergence factor* $= \frac{\|\mathrm{h}-\mathrm{h}_k\|}{\|\mathrm{h}-\mathrm{h}_{k+1}\|}$, *where* h_k *denotes the solution under grid size* 2^k.

In Figure 4, the convergence factor is plotted versus k. From the figure, we know that the solver to the forward problem has second order accuracy.

5.3 Results of inverse problem

If the regular term $\frac{\gamma}{2}\|\alpha\|^2_{L^2(\Omega_c)}$ is ignored, we recast the problem as a PDE-constraint optimization problem

$$\min J(h_m(\alpha), h_c(\alpha), \alpha) = \frac{1}{2}\|h_m - h_d^m\|^2_{L^2(\Omega_1)} + \frac{1}{2}\|h_c - h_d^c\|^2_{L^2(\Omega_2)},$$
$$\text{s.t.} \begin{cases} -\Delta h_m = -\alpha(h_m - h_c)\delta_{\Omega_c} + f_m & \text{in } \Omega_m, \\ -\dfrac{\mathrm{d}^2 h_c}{\mathrm{d}x^2} = \alpha(h_m|_{\Omega_c} - h_c) + f_c & \text{in } \Omega_c, \end{cases}$$

where h_d^m and h_d^c are the measured data, i.e., the exact solution of (5.1) with the target exchange rate function $2+\sin(\pi x)$. At every step of the iteration, $\Delta\alpha$ is chosen by Theorem 4.1. And

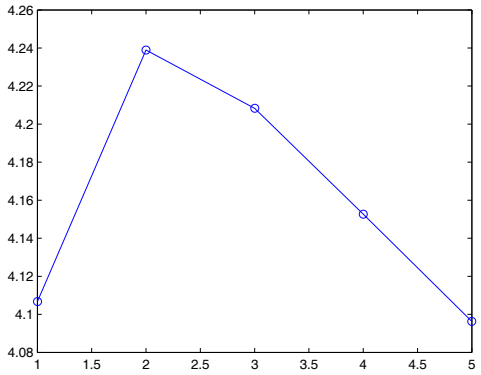

Figure 4 Convergence factor of finite difference approximation of h versus k for forward problem.

the initial guess of α is $y = 2$. The iteration stops when

$$\frac{|J(i) - J(i-1)|}{|J(i)|} < 10^{-5}$$

or the number of the iteration reaches the maximal step, where $J(i)$ denotes the energy of step i. The numerical results are sorted according to Ω_1 and Ω_2.

Case 1: $\Omega_1 = \{0\} \times [-1, 1]$, $\Omega_2 = \{0\}$, i.e., measured data on the left side of the boundary are given. Boundary conditions:

$$\begin{cases} \text{Neumann}, & \{0\} \times [-1, 1], \\ \text{Dirichlet}, & \text{else}. \end{cases}$$

Case 2: $\Omega_1 = \{0\} \times [-1, 1] \cup \{1\} \times [-1, 1]$, $\Omega_2 = \{0\} \cup \{1\}$, i.e., measured data on the left and right sides of the boundary are given. Boundary conditions:

$$\begin{cases} \text{Neumann}, & \Omega_1, \Omega_2, \\ \text{Dirichlet}, & \text{else}. \end{cases}$$

Case 3: For ideal case, $\Omega_1 = \Omega_m$, $\Omega_2 = \Omega_c$, i.e., all the measured data are given and the boundary condition is Dirichlet boundary condition.

Figures 5–7 correspond to Cases 1–3, respectively. Comparing these three results, we can find more accuracy of the unknown value if we know more information of the solutions. Specially for the Case 3 where the solutions are known in whole domain. Based on the results from Figure 7, it is hopeful to get one theoretical convergence analysis for the unknown α. But if only partially data (such as boundary values of the solutions) are measured as Case 1 and Case 2, the problems turn to be ill-posed, and it is hard to get enough accuracy.

Next, we discuss the case that the measured data are perturbed by noise. For the above three cases, we add $\pm 5\%$ noise to the measure data, the numerical results are reported in Figure 8 (Case 1), Figure 9 (Case 2) and Figure 10 (Case 3). In the cases with noises, these figures

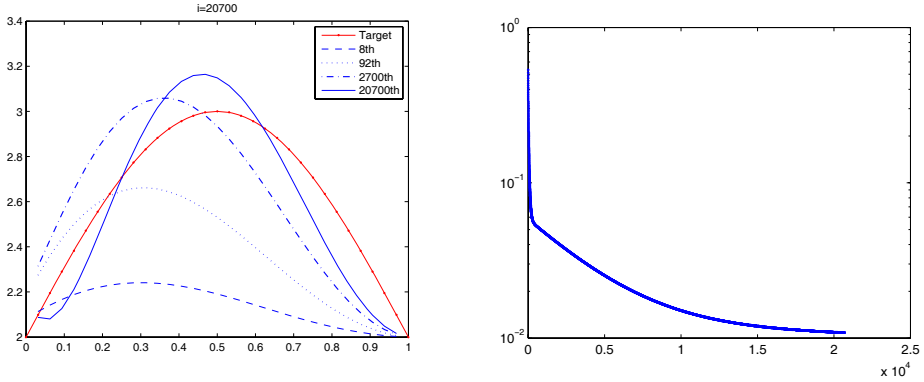

Figure 5 Iteration process (left) and log of the energy (right), $k = 5$, measured data of left side are known, iteration number is 20700.

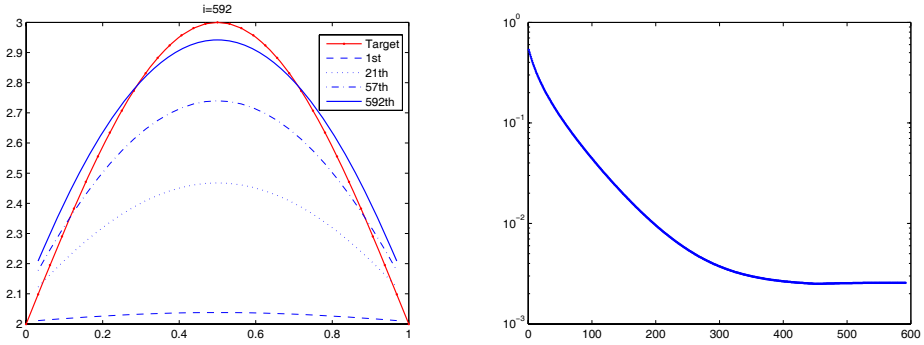

Figure 6 Iteration process (left) and log of the energy (right), $k = 5$, measured data of left and right sides are known, iteration number is 592.

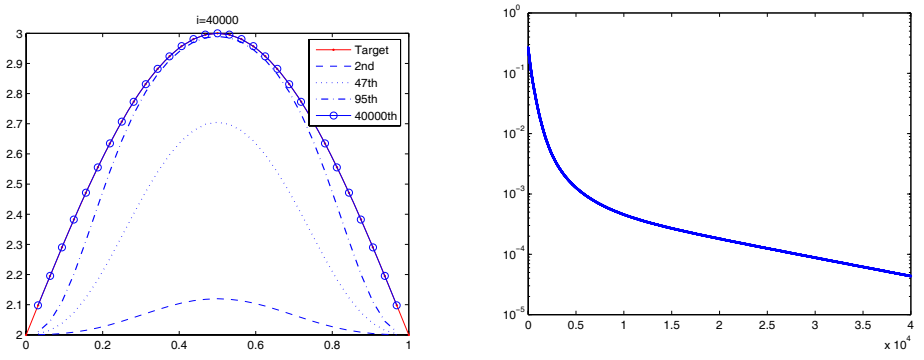

Figure 7 Iteration process (left) and log of the energy (right), $k = 5$, measured data of all the domain are known, iteration number is 40000.

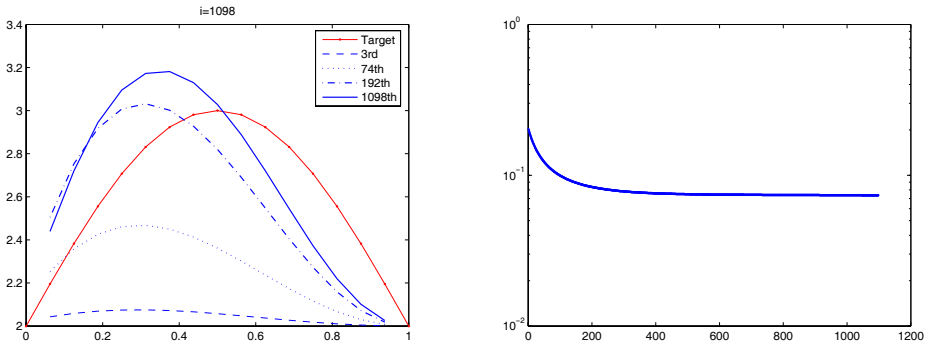

Figure 8 $k = 4$, measured data of left side are known, noise level: $\pm 5\%$, iteration number is 1098.

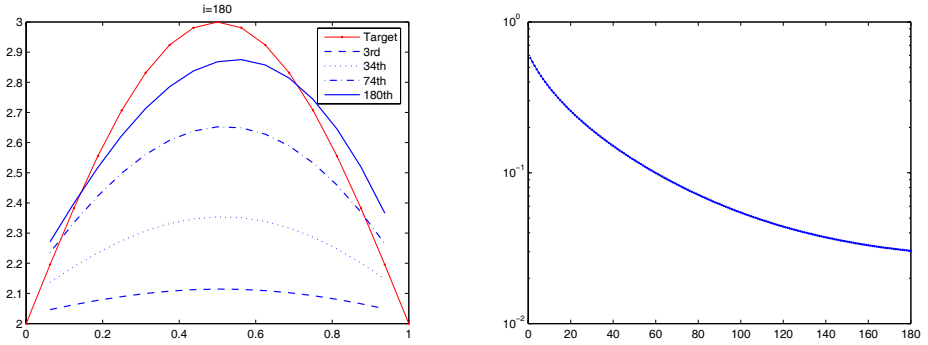

Figure 9 $k = 4$, measured data of left and right sides are known, noise level: $\pm 5\%$, iteration number is 1098.

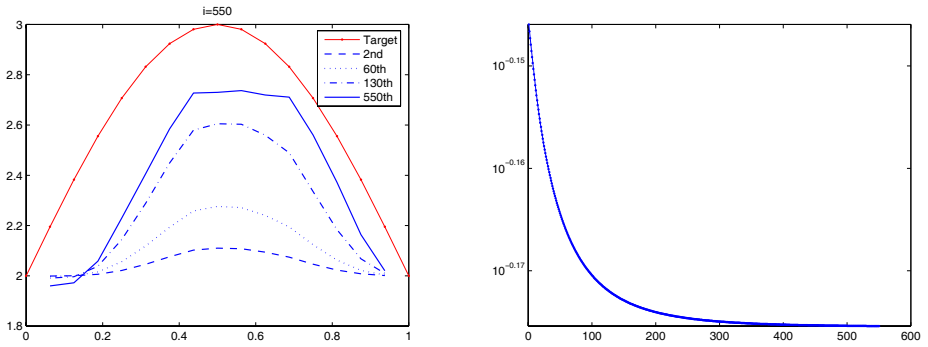

Figure 10 $k = 4$, measured data of all the domain are known, noise level: $\pm 5\%$, iteration number is 550.

show that the energy functional stagnates in the higher level than the cases without noises, while the inversion results can still be acceptable.

Acknowledgments The authors thank Xiaoming Wang, Neil Hua and Shuai Lu for their helpful discussions and suggestions.

References

[1] Adams, R. A., Sobolev Spaces, Academic Press, New York, 1975.

[2] Bauer, S., Liedl, R. and Sauter, M., Modeling of karst aquifer genesis: Influence of exchange flow, *Water Resour. Res.*, **39**(10), 2003, SBH6.1–SBH6.12.

[3] Bear, J. and Verrruijt, A., Modeling Groundwater Flow and Pollution, D. Reidel. Pub. Co., Norwell, Mass, 1987.

[4] Birk, S., Liedl, R., Sauter, M. and Teutsch, G., Hydraulic boundary conditions as a controllong factor in karst gensis: A numerical modeling study on artesian conduit development in gypsum, *Water Resour. Res.*, **39**(1), 2003, SBH2.1–SBH2.14.

[5] Bobok, E., Fluid Mechanics for Petroleum Engineers, Elservier Sci, New York, 1993.

[6] Bonnans, J. F., Gilbert, J. C., Lemarechal, C. and Sagastizabal, C. A., Numerical Optimization: Theoretical and Practical Aspects, 2nd Edition, Springer-Verlag, Berlin, 2006.

[7] Brandenburg, C., Lindemann, F., Ulbrich, M. and Ulbrich, S., A continuous adjoint approach to shape optimization for Navier-Stokes flow, Optimal Control of Coupled Systems of Partial Differential Equations, International Series of Numerical Mathematics, **158**, 2009, 35–56.

[8] Cao, Y., Gunzburger, M., Hua F. and Wang X., Analysis and finite element approximation of a coupled, continuum pipe-flow/Darcy model for flow in porous media with embedded conduits, *Numer. Math. PDE*, **27**(5), 2010, 1243–1252.

[9] Chen, N., Gunzburger, M., Hu, B., et al., Calibrating the exchange coefficient in the modified coupled continuum pipe-flow model for flows in karst aquifers, *J. Hydrol*, **414–415**, 2012, 294–301.

[10] Chen, W., Cheng, J., Lin, J. and Wang, L., A level set method to reconstruct the interface of discontinuity in the conductivity, *Science in China Series A: Mathematics*, **52**(1), 2009, 29–44.

[11] Feijóo, G. R., Malhotra, M., Oberai, A. A., et al., Shape sensitivity calculations for exterior acoustics problems, *Eng. Comput.*, **18**(3/4), 2001, 376–391.

[12] Feijóo, G. R., Oberai, A. A. and Pinsky, P. M., An application of shape optimization in the solution of inverse acoustic scattering problems, *Inverse Problems*, **20**(1), 2004, 199–228.

[13] Hinze, M., Pinnau, R., Ulbrich, M. and Ulbrich, S., Optimization with PDE Constraints, Springer-Verlag, Berlin, 2009.

[14] Hua, F., Modeling, analysis and simulation of Stokes-Darcy system with Beavers-Joseph interface condition, Ph.D. Thesis, Florida State University, Tallahassee, 2009.

[15] Liedl, R., Sauter, M., Hckinghaus, D., et al., Simulation of the development of Karst aquifers using a coupled continuum pipe flow model, *Water Resour. Res.*, **39**(3), 2003, SBH6.1–SBH6.11.

[16] Lu, S., Chen, N., Hu, B. and Cheng, J., On the inverse problems for the coupled continuum pipe flow model for flows in karst aquifers, *Inverse Problems*, **28**(6), 2012, 065003.

[17] Narasimhan, T. N., Multidimensional numerical simulation of fluid flow in fractured porous media, *Water Resour. Res.*, **18**(4), 1982, 1235–1247.

[18] Vogel, C. R., Computational methods for inverse problems, Frontiers in Applied Mathematics, SIAM, Philadelphia, 2002.

[19] Wang, X., On the coupled continuum pipe flow model (CCPF) for flows in Karst aquifer, *DCDS-B*, **13**(2), 2010, 489–501.